*Article*

# Gas-Phase Nucleophilic Reactivity of Alkoxysilanes

*Thiago C. Correra,[a] Luciano A. Xavier[a] and José M. Riveros\*,[a,b]*

*[a]Instituto de Química, Universidade de São Paulo, 13084-971 São Paulo-SP, Brazil*

*[b]Centro de Cîencias Naturais e Humanas, Universidade Federal do ABC, 09210-580 Santo André-SP, Brazil*

A reatividade em fase gasosa das alcoxissilanas do tipo $Me_{4-n}Si(OEt)_n$ (n = 1-3) foi investigada por ressonância ciclotrônica de íons por transformada de Fourier (FT-ICR) com o intuito de se caracterizar os mecanismos de ataque nucleofílico nesses importantes precursores de novos materiais. Nucleófilos como $F^-$, $MeO^-$ e $EtO^-$ reagem rapidamente e de forma preferencial atacando o átomo de Si, formando a espécie pentacoordenada de Si. Esta em seguida sofre processos de eliminação iniciados, ou por um íon metídio nascente $Me^-$, ou um íon etoxido $EtO^-$, que por sua vez, podem abstrair um próton gerando carbânions ou silóxidos. Carbânions do tipo $X(Me)_{3-n}Si(OEt)_nCH_2^-$ (X = F, MeO, EtO e n = 1-3) e silóxidos do tipo $X(Me)_{4-n}Si(OEt)_{n-1}O^-$ (X = F, MeO, EtO e n = 2-3) podem ser facilmente dissociados por excitação multifotônica no infravermelho induzida por um laser de $CO_2$ gerando uma grande variedade de silóxidos simples e silicatos análogos à espécies intermediárias encontradas nas primeiras etapas de processos sol-gel. Para as alcoxissilanas que contêm mais grupos etóxido, uma reação competitiva análoga a uma eliminação E2 é observada, onde o nucleófilo abstrai um hidrogênio β de um grupo etoxila, eliminando etileno. A cinética, distribuição relativa de produtos e termoquímica dessas reações também são apresentadas para alguns casos específicos.

The gas-phase reactivity of the $Me_{4-n}Si(OEt)_n$ (n = 1-3) alkoxysilanes was investigated by Fourier transform ion cyclotron resonance (FT-ICR) technique in order to characterize the fundamental mechanisms associated with nucleophilic attack on these important precursors of new materials. Typical nucleophiles such as $F^-$, $MeO^-$ and $EtO^-$ react readily and preferentially by attack at the silicon center with formation of a pentacoordinated siliconate that undergoes elimination processes initiated by either a nascent methide ion, Me, or an ethoxide ion, EtO, that can abstract a proton to yield either a carbanion or a siloxide-type anion. Carbanions of the type $X(Me)_{3-n}Si(OEt)_nCH_2^-$ (X = F, MeO, EtO and n = 1-3) and siloxide ion of the type $X(Me)_{4-n}Si(OEt)_{n-1}O^-$ (X = F, MeO, EtO and n = 2-3) can be easily dissociated by infrared multiphoton excitation with a $CO_2$ laser to give rise to a large variety of simple siloxide and silicate-type anions that are reminiscent of intermediate species in the early stages of sol-gel processes. For the higher-ethoxy containing substrates, a competing reaction is observed that is analogous to an E2 elimination reaction in which the nucleophile abstracts a β-proton from the ethoxy group leading to elimination of ethylene. The kinetics, relative product distribution and thermochemistry of these reactions are also reported for some specific cases.

**Keywords:** alkoxysilanes, nucleophilic reactivity, gas-phase ion chemistry, siliconates

## Introduction

The chemistry of alkoxysilanes has attracted considerable attention in the last 30 years because these substrates are: (*i*) notorious precursors of a wide variety
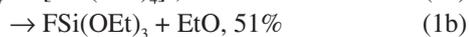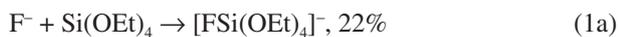
of hybrid materials[1-3] and (*ii*) the reagents of choice for deposition of silicon-containing thin films.[4-6] Thus, understanding the reactivity of these alkoxysilanes has been of primary interest in the search for tailor-made materials.[7]

A first-principle approach toward mapping out the fundamental reactivity of alkoxysilanes has relied on experiments within the realm of gas-phase ion chemistry under low-pressure conditions. Studies of this nature can often reveal valuable information on the intrinsic

reactivity and thermochemistry of these substrates. For example, some earlier work on the reactions of tetraalkoxysilanes with negatively charged nucleophiles showed that the predominant mechanism involves the initial formation of a pentacoordinated adduct followed by elimination processes.[8-10] This is illustrated in reaction 1 as characterized by ion cyclotron resonance techniques.

$$F^- + Si(OEt)_4 \rightarrow [FSi(OEt)_4]^-, 22\% \qquad (1a)$$
$$\rightarrow FSi(OEt)_3 + EtO, 51\% \qquad (1b)$$
$$\rightarrow FSi(OEt)_2O^- + [H_2O + C_2H_4], 27\% \quad (1c)$$

By comparison, the simple gas-phase reaction of nucleophiles with tetramethylsilane involves initial attack on the silicon center followed by elimination of a nascent carbanion as shown in reactions 2 and 3.[11-15]

$$F^- + Me_4Si \quad \rightarrow F(Me)_2SiCH_2^- + CH_4 \qquad (2)$$
$$OH^- + Me_4Si \quad \rightarrow Me_3SiO^- + CH_4 \qquad (3)$$
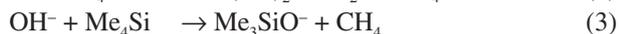
In spite of these early investigations, the gas-phase reactivity of alkoxysilanes has not been explored in a systematic way although some aspects of their reactivity have been explored by different experimental techniques.[16,17]

A more systematic study of the reactivity of alkoxysilanes toward simple nucleophiles was prompted by three present areas of interest: (*i*) the synthetic applications of these reactions;[18-20] (*ii*) the exact nature of the displacement reactions at silicon centers;[21-24] (*iii*) the increasing knowledge of thermochemical parameters of simple silicon species.[25-27] As part of our continuous interest in unraveling the intrinsic mechanisms of nucleophilic reactions in alkoxysilanes,[28,29] this manuscript describes the detailed gas-phase processes associated with the reaction of simple nucelophiles such as $F^-$, $MeO^-$ and $EtO^-$ with different ethoxysilanes, $Me_{4-n}Si(OEt)_n$ (n = 1-3). Our studies also extended to reactions with $O^-$ because of the potential interest in the outcome of these reactions in plasma enhanced vapor deposition (PECVD) processes.

## Experimental

The Fourier transform ion cyclotron resonance (FT-ICR) spectrometer and the typical operational conditions to characterize the gas-phase ion chemistry of metal alkoxides have been previously described.[30-33]

Fluoride ions were generated by dissociative electron attachment from $NF_3$ (Air Products) at pressures of $(1.5 \pm 0.5) \times 10^{-8}$ Torr (ion gauge reading). The electron energy was maintained at $-1.5$ eV and the trapping voltage at $-2.0$ V. Thermal electrons were ejected from the cell with a radio-frequency field of ca. 7 MHz applied to one of the trapping plates during the initial 140 ms of each acquisition cycle. $MeO^-$ and $EtO^-$ were generated from the corresponding alkyl nitrites at similar electron energies and pressures. The alkyl nitrites were prepared by alcoholysis of *n*-amyl nitrite prepared according to the procedure described by Noyes.[34] Finally, $O^-$ was obtained from $N_2O$ by dissociative electron attachment at similar electron energies.[35] The alkxoysilanes (Strem Chemicals) were used without further purification and their positive ion mass spectra revealed no noticeable impurities. The total pressure after introduction of the alkoxysilane was typically ca. $2.5 \times 10^{-8}$ Torr.

The kinetics of the different ion/molecule reactions were studied after isolation of the ion of interest through a combination of single frequency and swept frequency ejection pulses and by varying the trapping time prior to ion detection. Because our main interest was concentrated in the primary reaction products, only a few systems were studied at reaction times longer than 2.5 s.

Multiphoton infrared photodissociation experiments (IRMPD) were carried out using a grating tunable cw $CO_2$ laser (Lasertech Group, model LTG250 626G) and the general procedure described in the literature.[31]

### Computational details

The thermochemistry of several reactions described in this work, particularly those initiated by $F^-$, was calculated using the Gaussian03 suite of programs.[36] Structures were initially optimized using the common density functional B3LYP/6-31+G(d) and final structures and energies were then optimized and calculated at the B3LYP/6-311+G(3df, 2p) level.

## Results and Discussion

Fluoride ($F^-$) and methoxide ($MeO^-$) ions react rapidly with the ethoxysilanes to yield $EtO^-$ as the main and predominant reaction product. This is exemplified in reaction 4:

$$X^- (X = F, MeO) + Me_nSi(OEt)_{4-n} (n = 1-3) \rightarrow$$
$$F(Me)_nSi(OEt)_{3-n} + EtO^- \qquad (4)$$

While these reactions are moderately exothermic (Table 1), they occur via a facile displacement at the silicon center through a pentacoordinated intermediate.[22] These pentacoordinated siliconate type species, $[X(Me)_nSi(OEt)_{4-n}]^-$, can be observed in several cases as a minor stabilized product ion.

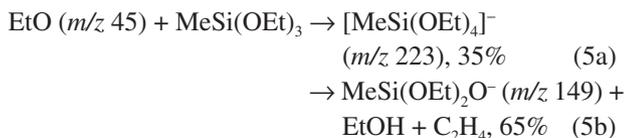**Table 1.** Calculated exothermicities at the B3LYP/6-311+G(3df, 2p) level for reaction 4 with $F^-$

|                              | $MeSi(OEt)_3$ | $Me_2Si(OEt)_2$ | $Me_3SiOEt$ |
| ---------------------------- | ------------- | --------------- | ----------- |
| $\Delta H$ / (kcal mol$^{-1}$) | –6.5          | –6.6            | –7.4        |

Because reaction 4 is the main reaction, and $EtO^-$ reacts further with the alkoxysilanes, a better understanding of the reactivity in these systems could only be obtained from experiments in which $EtO^-$ ions were continuously ejected from the ICR cell. Thus, it was also necessary to characterize initially the reactions of $EtO^-$, generated directly from ethyl nitrite, with each of the alkoxysilanes in order to eliminate possible contribution from incomplete ejection of $EtO^-$ ions at short reaction times.

### Reactions with MeSi(OEt)$_3$

#### EtO$^-$/MeSi(OEt)$_3$ system

$EtO^-$ was observed to react easily by two different channels as shown in reaction 5 along with the product distribution.

$$EtO\ (m/z\ 45) + MeSi(OEt)_3 \rightarrow [MeSi(OEt)_4]^-$$
$$(m/z\ 223),\ 35\%\quad (5a)$$
$$\rightarrow MeSi(OEt)_2O^-\ (m/z\ 149) +$$
$$EtOH + C_2H_4,\ 65\%\quad (5b)$$

The kinetics displayed in Figure 1a is typical of exothermic gas-phase ion/molecule reactions that proceed through a transition state located below the energy of the reactants.

Reaction 5a reveals the direct addition to silicon to yield a pentacoordinated siliconate species similar to that observed previously.[8] Detection of these stable siliconate species in our FT-ICR experiments is dependent on thermalization of the ions and the ability of the product ion to delocalize the exothermicity of the reaction along its internal energy modes. By comparison, it is proposed that reaction 5b, calculated to be 15.8 kcal mol$^{-1}$ exothermic, arises from abstraction of a β proton from one of the ethoxy groups of the neutral substrate followed by elimination of ethylene as outlined in Scheme 1.

This mechanism is formally similar to E2 type reactions that are commonly observed in gas-phase ion/molecule reactions.[37,38] While the sole observation of the ionic
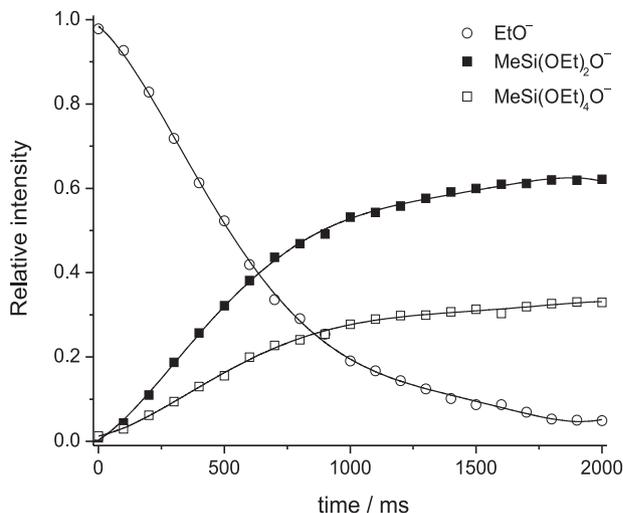


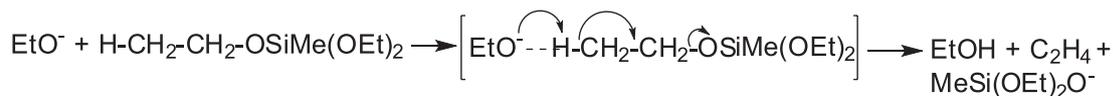**Figure 1.** Kinetics of reaction 5 under our typical experimental conditions.

product does not preclude the possibility of the reaction proceeding via nucleophilic substitution at the carbon center with formation of $Et_2O$ as the neutral product, previous experiments in these laboratories with ethyl esters reveal strong preference for the E2 mechanism.[39,40]
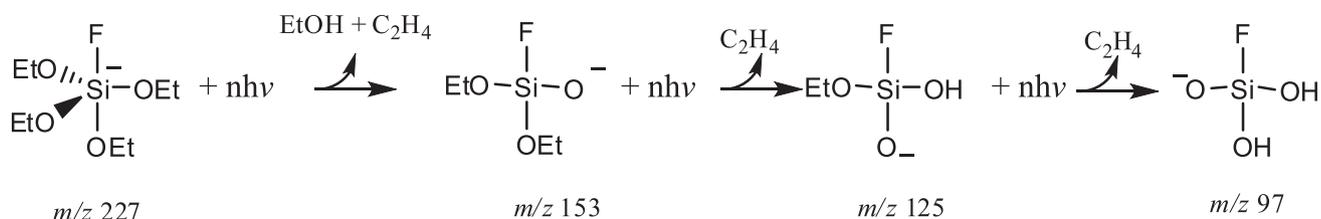
The possibility that reaction 5b is actually initiated by an $EtO^-$ originating from the energy-rich hypervalent siliconate species is an interesting question. Attempts to model these processes by computational model chemistry are still being under investigation because of the need of higher levels of theory to identify the transition state. On the other hand, an interesting experiment that is applicable to all the pentacoordinated species studied in this work adds some support to the idea that reaction 5b can also be promoted by activating the siliconate ion.

Scheme 2 shows the results of the sequential dissociation of a siliconate ion containing four ethoxy groups promoted by IRMPD.

This experiment clearly establishes that the lowest dissociation channel for these siliconate species is the release of a nascent ethoxide ion that proceeds to yield similar products to that of reaction 5b. Thus, it is not possible on the basis of our present experiments to distinguish whether the E2 process occurs by direct attack or via an activated siliconate intermediate. In principle, the use of either $C_2D_5O^-$ or $C_2H_5^{18}O^-$ as a reagent ion may shed some light on this question.

The sequential dissociation outlined in Scheme 2 follows the trend previously reported for alkoxy-containing

$$EtO^- + H\text{-}CH_2\text{-}CH_2\text{-}OSiMe(OEt)_2 \longrightarrow \left[ EtO^-\text{-}\text{-}H\text{-}CH_2\text{-}CH_2\text{-}OSiMe(OEt)_2 \right] \longrightarrow EtOH + C_2H_4 + MeSi(OEt)_2O^-$$

**Scheme 1**. E2-like mechanism proposed for reaction 5b.

**Scheme 2.** Sequential dissociation of the model siliconate $FSi(OEt)_4^-$ induced by IRMPD.

Ge and Ti oxyanions.[30,31] A particularly attractive feature of these IRMPD experiments is the ability to generate a variety of interesting anionic species as illustrated above. By analogy, sequential IRMPD of $MeSi(OEt)_2O^-$ yields the species shown in Scheme 3.

Two important features are particularly noticeable in the sequence shown in Schemes 2 and 3: (*i*) The mechanism for the sequential losses of ethylene can be easily accounted by a proton shift as shown in Scheme 4. This proton shift must be the lowest dissociation channel for these ions because no
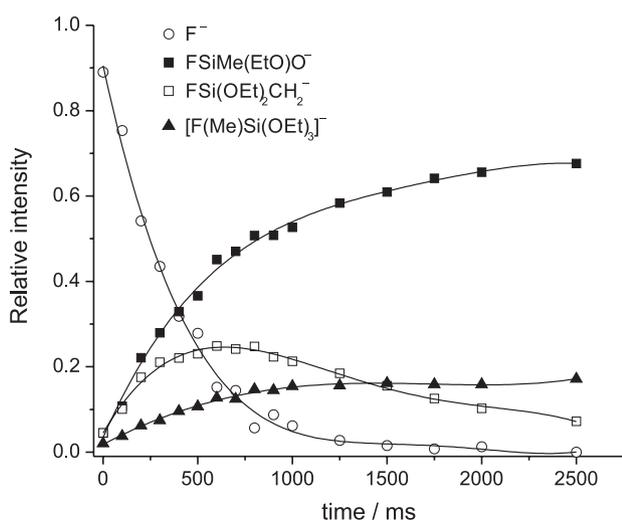


**Figure 2.** Kinetics of the $F^-$/$MeSi(OEt)_3$ reactions under continuous ejection of $EtO^-$ ions.

other competing IRMPD processes are observed; (*ii*) The sequential dissociation results in the progressive hydrolysis of the ethoxy groups attached to the silicon center and generate anions that are common species in the successive condensation reactions of sol-gel type processes. This ability is illustrated below for systems that were studied during longer reaction times.

### $F^-$/$MeSi(OEt)_3$ system

The detailed description of the reactions promoted by $EtO^-$ facilitates the interpretation of the results with the other nucleophiles. While $F^-$ reacts primarily through reaction 4, the reactions displayed in 6 are also readily observed.

$$F^- + MeSi(OEt)_3 \rightarrow [FSi(Me)(OEt)_3]^- \; (m/z\; 197),$$
$$\Delta H = -43 \text{ kcal mol}^{-1} \qquad (6a)$$
$$\rightarrow FSi(OEt)_2CH_2^- \; (m/z\; 151) + EtOH,$$
$$\Delta H = -3.1 \text{ kcal mol}^{-1} \qquad (6b)$$
$$\rightarrow FSi(Me)(OEt)O^- \; (m/z\; 123) + EtOH +$$
$$C_2H_4, \Delta H = -24.7 \text{ kcal mol}^{-1} \qquad (6c)$$
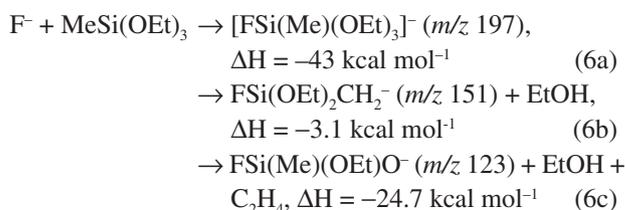
The kinetics of these reactions, under continuous ejection of $EtO^-$ ions, is shown in Figure 2.

Formation of a strong $F-Si$ bond in this case is reflected by the high exothermicity of the association reaction 6a. This value is consistent with the fluoride affinity of $Me_3SiOEt$ that was determined experimentally to amount to $31.4 \pm 1.2$ kcal mol$^{-1}$ from energy resolved dissociation
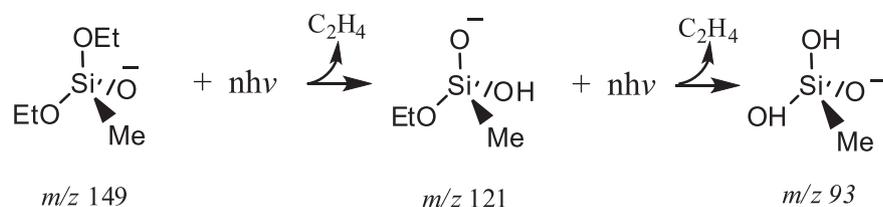


**Scheme 3**. Sequential IRMPD of $MeSi(OEt)_2O^-$ promoted induced by a $CO_2$ laser.
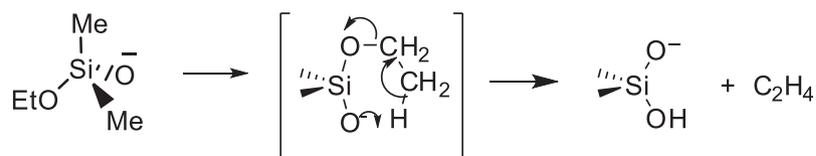


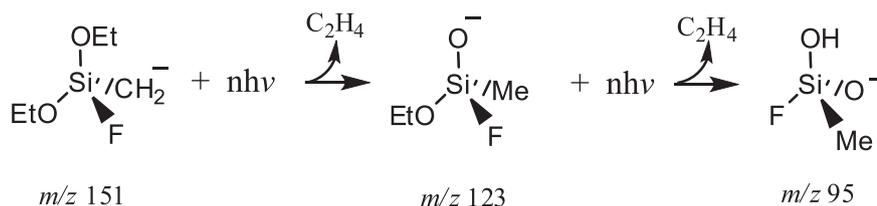**Scheme 4.** Proposed mechanism for the sequential loss of ethylene for the siloxide ions.

experiments of the pentacoordinated siliconate ions.[41] The strong tendency for $F^-$ to be attached to the Si center can in fact explain the different reactions shown above. Thus, the nascent $EtO^-$ of reaction 4 can either leave as an EtO or re-attack the neutral moiety $[F(EtO)_2SiCH_3]$ and abstract a proton from the methyl group to yield a carbanion (reaction 6b) similar to reaction 2. It is likely that a similar reaction is not observed for the $EtO^-$ because of the much lower stabilization of the siliconate species. Interestingly enough, formation of the $FSi(Me)(OEt)_3$ species is sufficiently exothermic that not only can reaction 6b be promoted but also the combined elimination of ethanol and ethylene can be observed in reaction 6c.

The connection between the product ions of reactions 6b and 6c can easily be observed in Figure 2. A decrease of $FSi(OEt)_2CH_2^-$ ($m/z$ 151) can be observed at longer reaction times while $FSi(Me)(OEt)O^-$ ($m/z$ 123) continues to increase. This is attributed to the unimolecular decomposition of the $m/z$ 151 ions promoted by the high temperature blackbody radiation emitted by the filament used in the ionization process. This phenomenon has been well characterized in our spectrometer for several cases.[42-44]
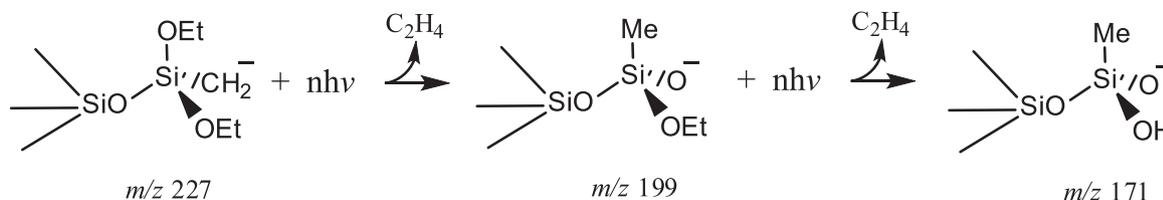
The sequential loss of ethylene units from the $m/z$ 151 ion was also followed by IRMPD techniques using a $CO_2$ laser as shown in Scheme 5.

The mechanism for the processes shown in Scheme 5 is similar to that outlined in Scheme 4 and the selective elimination of ethylene units again provides a unique gas-phase synthetic tool of a variety of substituted siloxide ions.
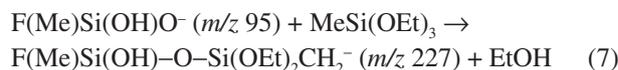
The final product shown in Scheme 5 was the subject of some further reactivity studies. This $F(Me)Si(OH)O$ ion can act as a nucleophile and undergo reaction 7 with the neutral substrate in an analogous fashion to reaction 6b.

$$F(Me)Si(OH)O^- \ (m/z\ 95) + MeSi(OEt)_3 \rightarrow$$
$$F(Me)Si(OH)-O-Si(OEt)_2CH_2^- \ (m/z\ 227) + EtOH \quad (7)$$

Sequential IRMPD dissociation of the $m/z$ 227 ion was again observed to proceed by consecutive elimination of ethylene units giving rise to a number of anions containing the siloxane core as shown in Scheme 6.

### $MeO^-/MeSi(OEt)_3$ system

This system displays a much richer reactivity pattern as shown in reaction 8. The quoted relative product distribution refers to the reactions under continuous ejection of $EtO^-$ ions.

$$MeO^- + MeSi(OEt)_3 \rightarrow [MeOSi(Me)(OEt)_3]^-$$
$$(m/z\ 209),\ 14\% \quad (8a)$$
$$\rightarrow MeOSi(OEt)_2O^- \ (m/z\ 165) +$$
$$CH_4 + C_2H_4,\ 19\% \quad (8b)$$
$$\rightarrow MeOSi(OEt)_2CH_2^- \ (m/z\ 163) +$$
$$EtOH,\ 19\% \quad (8c)$$
$$\rightarrow MeSi(OEt)_2O^- \ (m/z\ 149) +$$
$$MeOH + C_2H_4,\ 48\% \quad (8d)$$
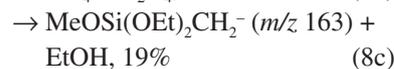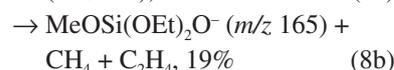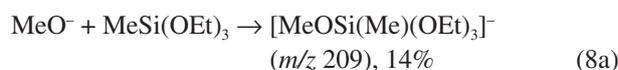
Reactions 8a-8c can again be envisioned as proceeding by initial formation of the pentacoordinated siliconate species ($m/z$ 209) followed by displacement of a nascent $Me^-$ as in reaction 2 and abstraction of a proton from an ethoxy group leading to the elimination of ethylene through reaction 8b. By analogy, reaction 8c can be attributed to a nascent $EtO^-$ that can either appear as a product (reaction 4) or abstract a proton selectively from the methyl group to yield a carbanion that is common in the reactions in silanes.[11,12] Finally, reaction 8d can be rationalized as an elimination-type reactions analogous to reaction 5b in



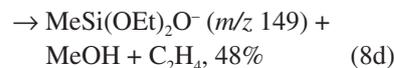**Scheme 5.** Sequential dissociation of $FSi(OEt)_2CH_2^-$ by IRMPD.



**Scheme 6.** Sequential dissociation of $F(Me)Si(OH)-O-Si(OEt)_2CH_2^-$ induced by IRMPD.

which the methoxide ion abstracts a proton directly from the ethoxy group followed by ethylene elimination.

Isolation of the major ionic product of reaction 8, namely $MeSi(OEt)_2O^-$, followed by IRMPD yields the same results outlined in Scheme 3. In this particular case, reaction of the final dissociation product, $MeSi(OH)_2O^-$, with the original neutral substrate reveals the addition-elimination type reaction similar to that shown in reaction 7.

### Reactions with $Me_2Si(OEt)_2$

The reactions and mechanisms that were extensively discussed above can be readily applied to the other alkoxysilanes.

### $EtO^-/Me_2Si(OEt)_2$ system

The reactions are outlined in 9 and the kinetics displayed in Figure 3. The most noticeable difference with respect to the reactions in $MeSi(OEt)_3$ is the fact that the presence of a second methyl group opens up reaction 9b. This is the result of a nascent $Me^-$ displaced from the siliconate ion ($m/z$ 193) abstracting a proton from the ethoxy group leading to elimination of ethylene.
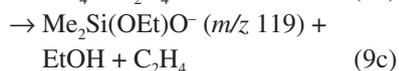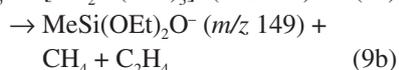
$$EtO^- + Me_2Si(OEt)_3 \rightarrow [Me_2Si(OEt)_3]^- \ (m/z \ 193) \quad (9a)$$
$$\rightarrow MeSi(OEt)_2O^- \ (m/z \ 149) +$$
$$CH_4 + C_2H_4 \quad (9b)$$
$$\rightarrow Me_2Si(OEt)O^- \ (m/z \ 119) +$$
$$EtOH + C_2H_4 \quad (9c)$$

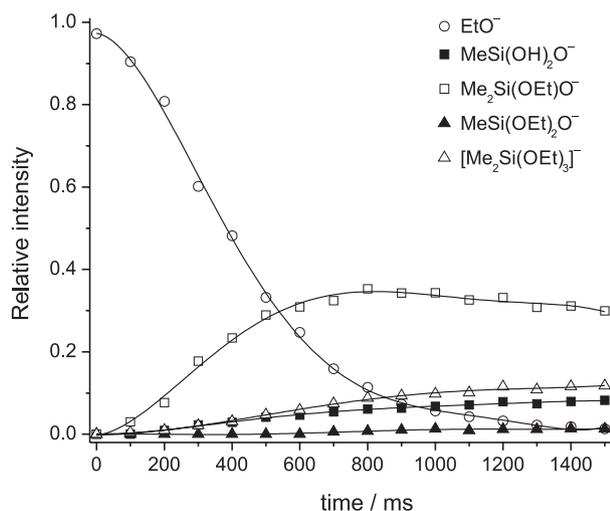Figure 3 also includes the kinetics of the $MeSi(OH)_2O^-$ ($m/z$ 93) that results from the sequential dissociation of

$MeSi(OEt)_2O^-$ induced by the infrared radiation of the filament as described above.

### $F^-/Me_2Si(OEt)_2$ system

The main reactions of this system, under continuous ejection of $EtO^-$ ions, are displayed in 10 along with the calculated exothermicities.
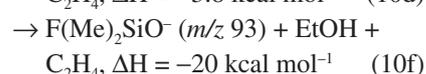
$$F^- + Me_2Si(OEt)_2 \rightarrow [FSi(Me)_2(OEt)_2]^- \ (m/z \ 167),$$
$$\Delta H = -37.5 \ \text{kcal mol}^{-1} \quad (10a)$$
$$\rightarrow F(Me)Si(OEt)_2CH_2^- \ (m/z \ 151) +$$
$$CH_4, \Delta H = -29.8 \ \text{kcal mol}^{-1} \quad (10b)$$
$$\rightarrow F(Me)Si(OEt)CH_2^- \ (m/z \ 121) +$$
$$EtOH, \Delta H = -0.3 \ \text{kcal mol}^{-1} \quad (10c)$$
$$\rightarrow Me_2Si(OEt)O^- \ (m/z \ 119) + HF +$$
$$C_2H_4, \Delta H = -3.8 \ \text{kcal mol}^{-1} \quad (10d)$$
$$\rightarrow F(Me)_2SiO^- \ (m/z \ 93) + EtOH +$$
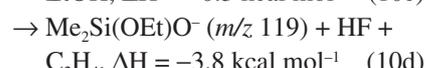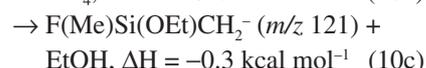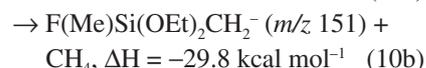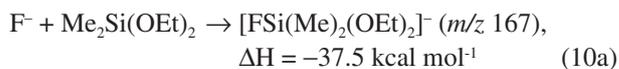$$C_2H_4, \Delta H = -20 \ \text{kcal mol}^{-1} \quad (10f)$$

Figure 4 displays the kinetics of the more important reactions in this system, and some of the actual mass spectra obtained at different reaction times are shown in Figure S1 in the Supplementary Information section. Subsequent dissociations promoted by infrared radiation of the filament are responsible for the variation of the product distribution. For example, EtO-containing ions such as the $m/z$ 121 and 151 ions undergo $C_2H_4$ elimination as observed in Figure 4. On the other hand, the kinetic behavior of $F(Me)_2SiO^-$ clearly suggests that this is not a primary reaction product but originating from dissociation of the $F(Me)Si(OEt)CH_2^-$ ($m/z$ 121) ion.

The general pattern observed is consistent with the different mechanisms discussed for $MeSi(OEt)_3$ with the



**Figure 3.** Kinetics of the reactions in the $EtO^-/Me_2Si(OEt)_2$ system.



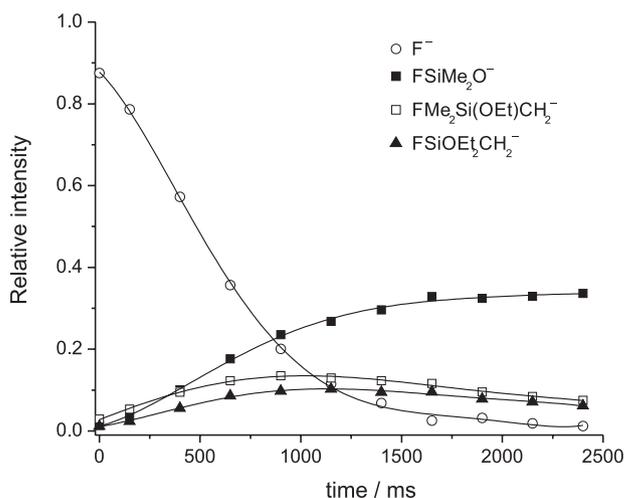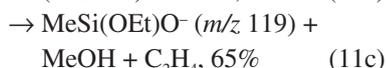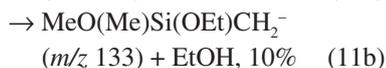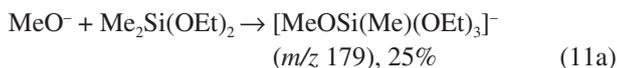**Figure 4.** Kinetics of the most important product ions for the $F^-/Me_2Si(OEt)_2$ system under continuous ejection of $EtO^-$ ions.

nucleophile initially attacking the silicon center. Subsequent fragmentation of the siliconate ion formed upon addition of the nucleophile can again give rise to either a nascent $Me^-$ or $EtO^-$ that abstracts a proton from the substrate.[45]

### $MeO^-/Me_2Si(OEt)_2$ system

The reactions observed with $MeO^-$ bear strong resemblance to those observed in reaction 8 and are shown in 11 (neglecting the main reaction that leads to displacement of $EtO^-$).

$$MeO^- + Me_2Si(OEt)_2 \rightarrow [MeOSi(Me)(OEt)_3]^-$$
$$(m/z\ 179),\ 25\% \qquad (11a)$$
$$\rightarrow MeO(Me)Si(OEt)CH_2^-$$
$$(m/z\ 133) + EtOH,\ 10\% \qquad (11b)$$
$$\rightarrow MeSi(OEt)O^-\ (m/z\ 119) +$$
$$MeOH + C_2H_4,\ 65\% \qquad (11c)$$

The elimination reaction initiated by abstraction of a proton from the ethoxy group, reaction 11c, is again the second most important reaction channel for the $MeO^-$ ion.

These ions can undergo further dissociation under $CO_2$ laser irradiation as illustrated in Scheme 7 for the $MeSi(OEt)O^-$ ion.

$$Me_2Si(OEt)O^- + nh\nu \xrightarrow{\ \ C_2H_4\ \ } Me_2Si(OH)O^-$$
$$m/z\ 119 \qquad\qquad\qquad m/z\ 91$$
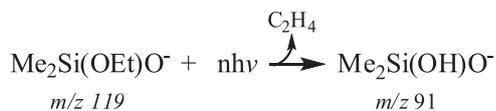
**Scheme 7.** Dissociation of $MeSi(OEt)O^-$ ions induced by IRMPD.

### Reactions with $Me_3SiOEt$

### $EtO^-/Me_3SiOEt$ system

As in the previous cases, the main reaction promoted by the $EtO^-$ results in the formation of a siloxide ion, $Me_3SiO^-$, from a reaction promoted by abstraction of a proton from the ethoxy group followed by ethylene elimination, reaction 12e below. Reactions originating from initial formation of a pentacoordinated siliconate species proceed either by methane elimination (see 12b below) or by elimination of ethanol (see reaction 12d) and are analogous to the reactions described for the other alkoxysilanes.

The full set of reactions observed for $EtO^-$ is displayed in 12, and the corresponding kinetics, including the minor reaction products, is shown in Figure 5.
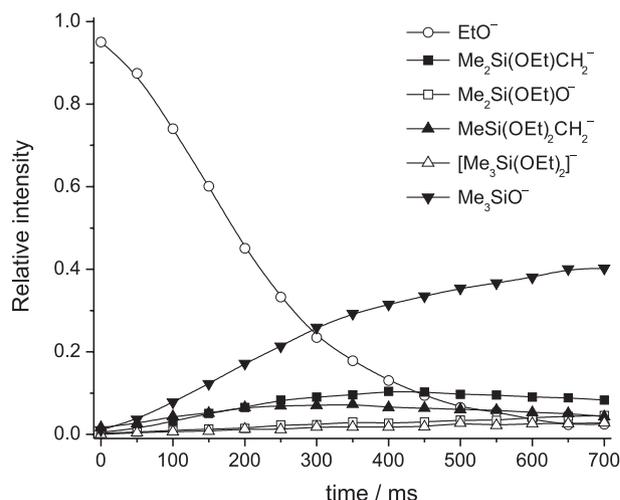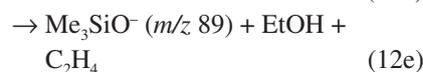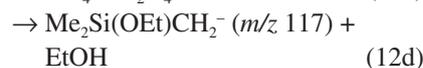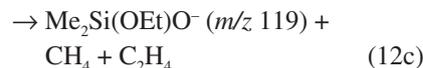
$$EtO^- + Me_3SiOEt \rightarrow [Me_3Si(OEt)_2]^-\ (m/z\ 163) \qquad (12a)$$
$$\rightarrow MeSi(OEt)_2CH_2^-\ (m/z\ 147) +$$
$$CH_4 \qquad (12b)$$

$$\rightarrow Me_2Si(OEt)O^-\ (m/z\ 119) +$$
$$CH_4 + C_2H_4 \qquad (12c)$$
$$\rightarrow Me_2Si(OEt)CH_2^-\ (m/z\ 117) +$$
$$EtOH \qquad (12d)$$
$$\rightarrow Me_3SiO^-\ (m/z\ 89) + EtOH +$$
$$C_2H_4 \qquad (12e)$$

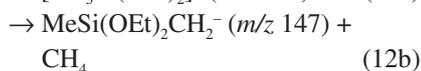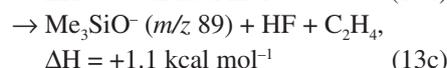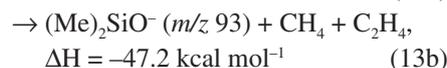**Figure 5.** Observed kinetics for the $EtO^-/Me_2Si(OEt)_2$ at relatively short reaction times.

Although Figure 5 emphasizes the early aspects of these reactions, the subsequent elimination of ethylene from $MeSi(OEt)_2CH_2^-$ and $Me_2Si(OEt)CH_2^-$ can be inferred from the kinetic behavior at longer reaction times.

### $F^-/Me_3SiOEt$ system

Under continuous ejection of $EtO^-$ ions, three main reactions are observed as outlined in 13 and in Figure 6.

$$F^- + Me_3SiOEt \rightarrow F(Me)Si(OEt)CH_2^-\ (m/z\ 121) + CH_4,$$
$$\Delta H = -27.65\ kcal\ mol^{-1} \qquad (13a)$$
$$\rightarrow (Me)_2SiO^-\ (m/z\ 93) + CH_4 + C_2H_4,$$
$$\Delta H = -47.2\ kcal\ mol^{-1} \qquad (13b)$$
$$\rightarrow Me_3SiO^-\ (m/z\ 89) + HF + C_2H_4,$$
$$\Delta H = +1.1\ kcal\ mol^{-1} \qquad (13c)$$

This system reveals that both $F(Me)_2Si(OEt)CH_2^-$ and $Me_3SiO^-$ are formed with similar rates at short reaction times. The fact that reaction 3c becomes very favorable is surprising in view of the fact that the elimination reaction is estimated to be slightly endothermic although the nucleophilic displacement resulting in the same $Me_3SiO^-$ ion and $C_2H_5F$ is calculated to be exothermic by $12.4\ kcal\ mol^{-1}$. This trend agrees with what is observed in the reactions with $EtO^-$ and points out that as the number of electronegative ligands attached to the silicon center, attack at the silicon becomes less favorable.
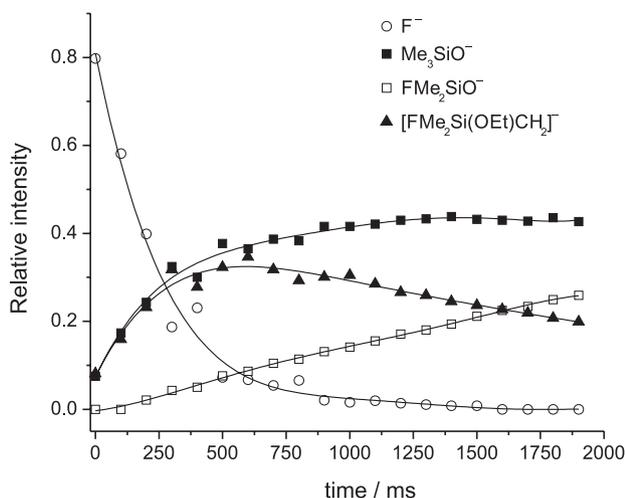
**Figure 6**. Kinetics recorded for the F⁻/Me₃SiOEt system under continuous ejection of EtO⁻.

Two other features should be emphasized for these reactions: (*i*) The decrease of $F(Me)_2Si(OEt)CH_2^-$ ions after 500 ms (Figure 6) is due to the same type of dissociation previously discussed that result in elimination of $C_2H_4$ and formation of the $F(Me)_2SiO$ (*m/z* 93) ion. Thus, an induction time is observed for the formation of $F(Me)_2SiO^-$ and these ions are not the products of a primary ion/molecule reactions. This dissociation was studied in details by isolating $F(Me)_2Si(OEt)CH_2^-$ ions after 500 ms and following the formation $F(Me)_2SiO$ as shown in Figure 7; (*ii*) A second important aspect of this system is that $Me_3SiO^-$ can slowly undergo sequential methyl-fluorine exchange with $NF_3$ (used to generate F⁻) as described in a recent report.[29] This process is responsible for the progressive appearance of $F_2MeSiO^-$ and $F_3SiO^-$ ions at long reaction times.
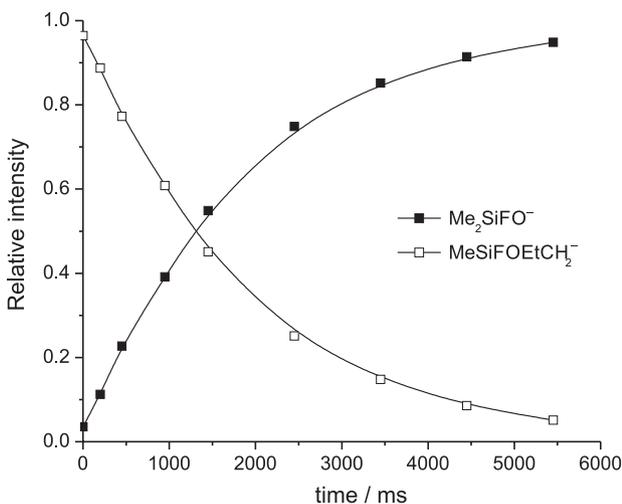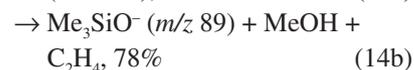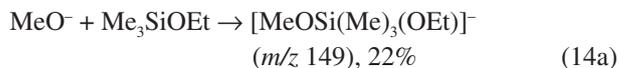


**Figure 7.** Kinetics of the dissociation of $F(Me)Si(OEt)CH_2^-$ induced by the infrared blackbody radiation emitted by the ionizing filament and formation of $Me_2Si(F)O^-$.

## MeO⁻/Me₃SiOEt system

This system displays a very simple pattern that is shown in 14

$$MeO^- + Me_3SiOEt \rightarrow [MeOSi(Me)_3(OEt)]^-$$
$$(m/z\ 149),\ 22\% \qquad (14a)$$
$$\rightarrow Me_3SiO^-\ (m/z\ 89) + MeOH +$$
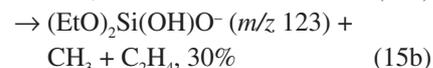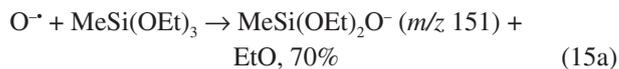$$C_2H_4,\ 78\% \qquad (14b)$$

As for the other nucleophiles, the reaction that proceeds by abstraction of a proton and ethylene elimination becomes the dominant reaction under continuous ejection of EtO⁻ ions. This reinforces the idea that this particularly channel becomes progressively more important as the number of ethoxy groups decreases in these alkoxysilanes.

## Reactions of O⁻

Reactions of O⁻ are interesting for a variety of reasons. In the case of alkoxysilanes, these reactions are particularly relevant for understanding some fundamental processes in PECVD. O⁻ can act both as a nucleophile and as a radical species and therefore its reactivity may reflect some differences with respect to the nucleophiles studied above.

A typical example is shown in reaction 15 for $MeSi(OEt)_3$ in which nucleophilic type reactions are observed and the neutral product is a radical.

$$O^{-\bullet} + MeSi(OEt)_3 \rightarrow MeSi(OEt)_2O^-\ (m/z\ 151) +$$
$$EtO,\ 70\% \qquad (15a)$$
$$\rightarrow (EtO)_2Si(OH)O^-\ (m/z\ 123) +$$
$$CH_3 + C_2H_4,\ 30\% \qquad (15b)$$

Both reactions are consistent with initial attack of the radical anion on the silicon followed by processes that are very similar to those observed for the other nucleophiles.

For all the alkoxysilanes, the reactions result in the formation of a closed shell anion and displacement of a neutral radical.

## Conclusions

The gas-phase reaction of simple nucleophiles with ethoxymethylsilanes has been shown to proceed primarily by an addition-elimination mechanism in which the nucleophile initially becomes attached to the silicon center. Under the low pressure conditions of the ion cyclotron resonance experiments, the exothermicity associated with the formation of the intermediate siliconate species is responsible for the direct displacement of nascent ethoxide ion or a methide ion that can abstract a proton to yield

either a carbanion or a siloxide-type anion. The preferred route for displacement depends on the exact number of methyl and ethoxy groups present and these groups can actually modulate the overall reactivity.

Sequential infrared multiphoton induced dissociation of the product ions can be used to generate a large number of simple siloxide and silicate-type anions that are usually involved in the early stages of hydrolysis and condensation reaction of sol-gel processes.

The present study shows that the actual nature of the reaction products can be conveniently selected by a suitable choice of nucleophile and the corresponding alkoxysilane and could provide a bottom up approach toward understanding the polymerization processes of alkoxysilanes in basic media.

## Supplementary Information

Supplementary data are available free of charge at http://jbcs.sbq.org.br as PDF file.

## Acknowledgements

## References

1. Hoffman, F.; Fröba, M.; *Chem. Soc. Rev.* **2011**, *40*, 608 and references therein.

2. Fujita, S.; Inagaki, S.; *Chem. Mater.* **2008**, *20*, 891.

3. Sanchez, C.; Soler-Illia, G. J. de A. A.; Ribot, F.; Lalot, T.; Mayer, C. R.; Cabuil, V.; *Chem. Mater.* **2001**, *13*, 3061.

4. Zhang, J.; Wavhal, D.; Fisher, E. R.; *J. Vac. Sci. Technol., A* **2004**, *22*, 201.

5. Bogart, K. H. A.; Ramirez, S. K.; Gonzales, L. A.; Bogart, G. R.; Fisher, E. R.; *J. Vac Sci. Technol., A* **1998**, *16*, 3175.

6. Ray, S. K.; Maiti, C. K.; Lahiri, S. K.; Chakrabarti, N. B.; *Adv. Mater. Opt. Electron.* **1996**, *6*, 73.

7. Corriu, R. J. P.; *Eur. J. Inorg. Chem.* **2001**, 1109.

8. da Silva; M. L. P.; Riveros, J. M.; *J. Mass Spectrom.* **1995**, *30*, 733.

9. Murthy, V. S.; Miller, J. M.; *Inorg. Chem.* **1995**, *34*, 4513.

10. Morgon, N. H.; Argenton, A. B.; da Silva, M. L. P.; Riveros, J. M.; *J. Am. Chem. Soc.* **1997**, *119*, 1708.

11. DePuy, C. H.; Bierbaum, V. M.; Flippin, L. A.; Grabowski, J. J.; King, G. K.; Schmitt, R. J.; Sullivan, S. A.; *J. Am. Chem. Soc.* **1980**, *102*, 5012.

12. Damrauer, R.; *Organometallics* **2004**, *23*, 1462.

13. DePuy, C. H.; Bierbaum, V. M.; Damrauer, R.; *J. Am. Chem. Soc.* **1984**, *106*, 4051.

14. DePuy, C. H.; Gronert, S.; Barlow, S. E.; Bierbaum, V. M.; Damrauer, R.; *J. Am. Chem. Soc.* **1989**, *111*, 1968.

15. Sheldon, J. C.; Hayes, R. N.; Bowie, J. H.; *J. Chem. Soc., Perkin Trans 2* **1987**, 275.

16. van der Wel, H.; Nibbering, N. M. M.; Sheldon, J. C.; Hayes, R. N.; Bowie, J. H.; *J. Am. Chem. Soc.* **1987**, *109*, 5823.

17. Damrauer, R.; Krempp, M.; *Organometallics* **1990**, *9*, 999.

18. Jorapur, Y. R.; Shimada, T; *Synlett* **2012**, *23*, 1064.

19. Allen, J. M.; Aprahamian, S. L.; Sans, E. A.; Schechter, H.; *J. Org. Chem.* **2002**, *67*, 3561.

20. Farooq, O.; *J. Fluorine Chem.* **1997**, *86*, 189.

21. O'Hair, R. A. J.; Bowie, J. H.; *Rapid Commun. Mass Spectrom.* **1989**, *3*, 10.

22. Bento, A. P.; Bickelhaupt, F. M.; *J. Org. Chem.* **2007**, *72*, 2201.

23. Yang, Z-Z.; Ding, Y-L.; Zhao, D-X.; *J. Phys. Chem. A* **2009**, *113*, 5432.

24. Kessler, V. G.; Spijksma, G. I.; Seisenbaeva, G. A.; Hakansson, S.; Blank, D. H. A.; Bouwmeester, H. J. M.; *J. Sol-Gel Sci. Technol.* **2006**, *40*, 163.

25. Liu, M.; Tran, N. T.; Franz, A. K.; Lee, J. K.; *J. Org. Chem.* **2011**, *76*, 7186.

26. Damrauer, R.; Simon, R.; Krempp, M.; *J. Am. Chem. Soc.* **1991**, *113*, 4431.

27. Damrauer, R.; Hankin, J. A.; *Chem. Rev.* **1995**, *95*, 1137.

28. Rainone, R.; Malaspina, T.; Xavier, L. A.; Riveros, J. M.; *Eur. J. Mass Spectrom.* **2010**, *16*, 379.

29. Correra, T. C.; Riveros, J. M.; *Angew. Chem., Int. Ed.* **2012**, *51*, 8632.

30. Xavier, L. A.; Malaspina, T.; Morgon, N. H.; Riveros, J. M.; *Int. J. Mass Spectrom.* **2011**, *306*, 219.

31. Xavier, L. A.; Riveros, J. M.; *Can. J. Chem.* **2005**, *83*, 1913.

32. Xavier, L. A.; Morgon, N. H.; Menegon, J. J.; Riveros, J. M.; *Int. J. Mass Spectrom.* **2002**, *219*, 485.

33. Morgon, N. H.; Xavier, L. A.; Riveros, J. M.; *Int. J. Mass Spectrom.* **2000**, *195/196*, 363.

34. Noyes, W. A.; *Org. Synth.* **1943**, *2*, 108.

35. Staneke, P. O.; Kauw, J.; Born, M.; Ingemann, S.; Nibbering, N. M. M.; *Rapid Commun. Mass Spectrom.* **1997**, *11*, 124.

36. Frisch, M. J. Frisch, M. J.; Trucks, G. W.; Schlegel, H. B.;

Scuseria, G. E.; Robb, M. A.; Cheeseman, J. R.; Montgomery, J. A.; Vreven, T.; Kudin, K. N.; Burant, J. C.; Millam, J. M.; Iyengar, S. S.; Tomasi, J.; Barone, V.; Mennucci, B.; Cossi, B.; Scalmani, G.; Rega, N.; Petersson, G. A.; Nakatsuji, H.; Hada, M.; Ehara, M.; Toyota, K.; Fukuda, R.; Hasegawa, J.; Ishida, M.; Nakajima, T.; Honda, Y.; Kitao, O.; Nakai, H.; Klene, M.; Li, X.; Knox, J. E.; Hratchian, H. P.; Cross, J. B.; Adamo, C.; Jaramillo, J.; Gomperts, R.; Stratmann, R. E.; Yazyev, O.; Austin, A. J.; Cammi, R.; Pomelli, C.; Ochterski, J. W.; Ayala, P. Y.; Morokuma, K.; Voth, G. A.; Salvador, P.; Dannenberg, J. J.; Zakrzewski, J.; Dapprich, S.; Daniels, A. D.; Strain, M. C.; Farkas, O.; Malick, D. K.; Rabuck, A. D.; Raghavachari, K.; Foresman, J. B.; Ortiz, J. V.; Cui, Q.; Baboul, A. G.; Clifford, S.; Cioslowski, J.; Stefanov, B. B.; Liu, G.; Liashenko, A.; Piskorz, P.; Komaromi, I.; Martin, R. L.; Fox, D. J.; Keith, T. J.; Al-Laham, M. A.; Peng, C. Y.; Nanayakkara, A.; Challacombe, M.; Gill, P. M. W.; Johnson, B.; Chen, W.; Wong, M. W.; Gonzalez, C.; Pople, J. A.; Gaussian 03, Revision E.01 ed.; Gaussian, Inc.: Pittsburgh, PA, USA, 2004.

37. Villano, S. M.; Eyet, N.; Lineberger, W. C.; Bierbaum, V. M.; *J. Am. Chem. Soc.* **2009**, *131*, 8227.

38. Gronert, S.; *Acc. Chem. Res.* **2003**, *36*, 848.

39. Correra, T. C.; Riveros, J. M.; *J. Phys. Chem A.* **2010**, *114*, 11910.

40. Takashima, K.; Riveros, J. M.; *J. Am. Chem. Soc.* **1978**, *100*, 6128.

41. Krouse, I. H.; Wenthold, P. G.; *J. Am. Soc. Mass Spectrom.* **2005**, *16*, 697.

42. Sena, M; Riveros, J. M.; *J. Phys. Chem.* **1997**, *101*, 4384.

43. Sena, M; Riveros, J. M.; *Int. J. Mass Spectrom.* **2003**, *227*, 135.

44. Giroldo, T; Riveros, J. M.; *J. Phys. Chem. A* **2002**, *106*, 9930.

45. For a thorough discussion of the mechanisms of siliconate anion fragmentation see: Krouse, I. H.; Wenthold, P. G.; *Organometallics* **2004**, *23*, 2573.